Res Chem Intermed (2016) 42:5013–5025
DOI 10.1007/s11164-015-2342-5

Microwave-assisted rapid synthesis of cerium phosphates and their adsorption on uranium(VI)

Rui Wang[1] · **Junwei Ye**[1] · **Guiling Ning**[1] ·
Fuhong Sun[2] · **Heng Jiang**[2] · **Xiaomeng Wu**[2] ·
Hongxue Liu[2]

Received: 26 June 2015 / Accepted: 26 October 2015 / Published online: 21 November 2015
© Springer Science+Business Media Dordrecht 2015

Abstract Cerium phosphates have been successfully synthesized under microwave irradiation in the absence of organic solvent. The effects of different molar ratios of phosphoric acid (85 %) to cerium hydroxide on the product phosphates were investigated. A single-phase CeP_2O_7 compound and a mixture of tetravalent cerium pyrophosphate (CeP_2O_7) and metaphosphate ($Ce(PO_3)_4$) were synthesized at 800 W for 5 min under microwave irradiation when the mole ratio of H_3PO_4 to $Ce(OH)_4$ was equal to 2 and 2.5–4, respectively. In the presence of chemometric excess of H_3PO_4 (mole ratio of H_3PO_4 to $Ce(OH)_4$ is between 5 and 6), a single-phase $Ce(PO_3)_4$ compound can be prepared at 480 W for 10 min under microwave irradiation. Scanning and transmission electron microscope images showed that particle sizes of CeP_2O_7 and $Ce(PO_3)_4$ were 0.1–3 and 1–5 μm, respectively. The adsorption properties of CeP_2O_7 and $Ce(PO_3)_4$ on uranium(VI) were examined. In the same condition, uranium(VI) was removed by $Ce(PO_3)_4$ more effectively than CeP_2O_7, and there are greater advantages for products synthesized under microwave irradiation than those calcination products on adsorption of uranium(VI).

Keywords Microwave irradiation · Cerium phosphates · Adsorption · Uranium

---

✉ Guiling Ning
ninggl@dlut.edu.cn

✉ Heng Jiang
hjiang78@hotmail.com

[1] State Key Laboratory of Fine Chemicals, School of Chemical Engineering, Dalian University of Technology, Dalian 116024, China

[2] School of Chemistry and Materials Science, Liaoning Shihua University, Fushun 113001, China

Introduction

In recent years, considerable attention has been paid to rare earth phosphates because of their applications in novel functional materials, such as fluorescence materials [1, 2], proton conductors [3–6], catalysts [7–10], magnetic cooling material [11], sunscreen materials [12–14], negative thermal expansion materials [15, 16], and efficient adsorbents for radwaste [17–19]. Several phosphates such as $Zr_2O(PO_4)_2$, ZrP_2O_7 and $Th_4(PO_4)_4P_2O_7$ have been studied as potential substitutes for immobilization and long-term storage of uranium [18]. Phosphates, especially rare earth phosphates, have poor solubility, strong irradiation resistance, excellent thermal stability, good binding ability with actinide elements, and high adsorption capability on actinide elements and heavy metals [15–28]. For this reason, rare earth phosphates as adsorbents are expected to play a significant role in the safety of underground radwaste repositories due their potential use for an engineered containment barrier. Therefore, more rare earth phosphates should be applied in adsorption of Uranium(VI) [U(VI)] so as to provide strong support for underground nuclear waste disposal. To the best of our knowledge, there is no literature reported about the adsorption properties of tetravalent cerium pyrophosphate (CeP_2O_7) and metaphosphate ($Ce(PO_3)_4$) on U(VI).

CeP_2O_7 and $Ce(PO_3)_4$ are difficult to obtain, and many resources are wasted because of their required harsh synthesis condition. Only a conventional calcination technique has been used to prepare CeP_2O_7 and $Ce(PO_3)_4$ in previous studies [3, 7, 8, 15, 29–31]. CeP_2O_7 powder can reportedly be obtained by the dehydration of $Ce(HPO_4)_2 \cdot xH_2O$, which was prepared by heating H_3PO_4 and $Ce(SO_4)_2 \cdot xH_2O$ under reflux conditions, using a heat treatment at 600 °C for 16 h. CeO_2 and 85 % H_3PO_4 have also been calcined at 300 °C for 8 h [3], or at 700 °C for 20 h [29]. Amorphous CeP_2O_7 powder has been obtained as well using $Ce(SO_4)_2 \cdot 4H_2O$ and $Na_4P_2O_7$ as initial materials at 80 °C for 24 h; crystallization from the amorphous phase occurred at around 500 °C to form crystalline cerium pyrophosphate [30]. Regarding $Ce(PO_3)_4$, it can reportedly be obtained by calcining CeO_2 and 85 % H_3PO_4 at 700 °C for 20 h [7, 31], or at 500 °C for longer than 6 h [27]. These calcination methods are time-consuming, resource-wasteful, and require high temperatures. Thus, a new and rapid synthesis route for CeP_2O_7 and $Ce(PO_3)_4$ should be required. In the current study, CeP_2O_7 and $Ce(PO_3)_4$ are directly synthesized using only microwave (MW) irradiation in the absence of any organic solvent, and are then applied as new mediums of U(VI)-sorption/fixation for radioactive liquid wastes processing.

Experimental

CeP_2O_7 and $Ce(PO_3)_4$ powders were synthesized using phosphoric acid (H_3PO_4; 85.0 % by weight) and cerium hydroxide ($Ce(OH)_4$; 99.9 %) at different mole ratios [$R = 2$, 2.5, 3, 4, 5, 5.5, 6, and 7, where R is the mole ratio of H_3PO_4 to $Ce(OH)_4$]. Different amounts of 85 % H_3PO_4 and 0.01-mol $Ce(OH)_4$ were adequately mixed in an agate mortar. The mixture was stored in a porcelain crucible with an insulation layer and directly irradiated at various MW powers for different times. The resultant powders were sufficiently washed with distilled water, and then dried at 60 °C for 1.5 h. For comparison, the reactions were also investigated by a high-temperature calcination method in a temperature-programmed muffle furnace when *R* was equal to 2, 4, and 5.

The equilibration of CeP_2O_7 or $Ce(PO_3)_4$ with uranyl ions was done by a batchwise operation. 0.02 g of CeP_2O_7 or $Ce(PO_3)_4$ was taken into a sealable Teflon tube ample at 25 °C for a certain time together with 20 mL of aqueous solution containing 2–5 mL of 4-mmol L^{-1} uranyl nitrate [$UO_2(NO_3)_2 \cdot 6H_2O$] solution (in 0.1-M HNO_3), 2 mL of 0.1-M KNO_3 solution, and 0.1-M KOH solution adjusted to pH values of 2–7. After U(VI) solutions were centrifuged at 3000 rpm for 15 min, the U(VI) concentration in the upper layer was determined spectrophotometrically using a arsenazo-III method [32, 33]. The effects of pH value, contact time, and initial concentrations of uranyl ions on U(VI) adsorption were studied.

MW irradiation was carried out using a MW oven (Galanz GB80)with a frequency of 2450 MHz and several power level settings up to a maximum output power of 800 W. The structure of products was confirmed by powder XRD using a D/MAX–RB X-ray diffractometer (Rigaku, Japan) with a graphite monochromator and Cu *Kα* radiation (40 kV, 100 mA). The step scan mode was used with a step width of 0.02°, at a rate of 4° (2θ) min^{-1}, in the scan range 10–70°. Phase indexing was performed using MDI Jade 6.5 software. Scanning electron microscope (SEM, JSM–7500F–EDS) observations were made using a Hitachi S–4800 microscope operated at 0.5 kV. High-resolution morphology and selected-area electron diffraction (SAED) were performed using transmission electron microscopy (TEM, JEOL–2100). The samples were dispersed on a carbon-coated copper grid for TEM observation. The uranium content was determined using a visible light spectrophotometer (722S Vis) at 652 nm for the U(VI)–arsenazo(III) complex against a reagent blank as the reference.

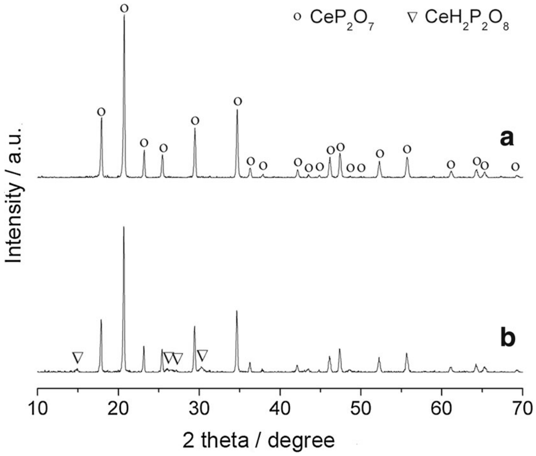

Fig. 1 XRD patterns of samples synthesized at 800 W for different times when $R = 2$. *a* 5 min (entry 2), *b* 3 min (entry 1)

Table 1 The results of the reaction between H_3PO_4 and $Ce(OH)_4$ under different conditions and removal rates of U(VI) from aqueous solutions using the obtained products as adsorbents

Entries	MW/Calcination condition		*R* value	Products	U(VI) removal rate (%)
1	MW	800 W 3 min	2	CeP_2O_7 containing a small amount of $CeH_2P_2O_8$	–
2	MW	800 W 5 min	2	CeP_2O_7	60.27
3	Calcination	260 °C 60 min	2	CeP_2O_7 containing a small amount of Ce_2O_3	–
4	Calcination	300 °C 60 min	2	CeP_2O_7	25.03
5	MW	800 W 5 min	2.5	CeP_2O_7 containing a small amount of $Ce(PO_3)_4$	64.91
6	MW	800 W 5 min	3	CeP_2O_7 and $Ce(PO_3)_4$	66.05
7	MW	800 W 3 min	4	$Ce(PO_3)_4$ containing a small amount of CeP_2O_7	–
8	MW	800 W 5 min	4	$Ce(PO_3)_4$ containing a small amount of CeP_2O_7	85.16
9	MW	800 W 10 min	4	$Ce(PO_3)_4$ containing a small amount of CeP_2O_7	–
10	MW	640 W 5 min	4	$Ce(PO_3)_4$ containing a small amount of CeP_2O_7	–
11	MW	640 W 10 min	4	$Ce(PO_3)_4$ containing a small amount of CeP_2O_7	–
12	Calcination	300 °C 60 min	4	CeP_2O_7	25.85
13	Calcination	300 °C 180 min	4	$Ce(PO_3)_4$ containing a small amount of impurities	–
14	Calcination	500 °C 180 min	4	$Ce(PO_3)_4$ containing a small amount of impurities	–
15	MW	800 W 5 min	5	$Ce(PO_3)_4$ containing a trace amount of CeP_2O_7	85.88
16	MW	800 W 10 min	5	$Ce(PO_3)_4$ containing a small amount of CeP_2O_7	–
17	MW	640 W 10 min	5	$Ce(PO_3)_4$	95.59
18	MW	560 W 10 min	5	$Ce(PO_3)_4$	96.25
19	MW	480 W 10 min	5	$Ce(PO_3)_4$	96.12
20	Calcination	300 °C 180 min	5	$Ce(PO_3)_4$ containing a small amount of impurities	–
21	Calcination	500 °C 180 min	5	$Ce(PO_3)_4$	37.32
22	MW	640 W 10 min	5.5	$Ce(PO_3)_4$	94.78
23	MW	560 W 10 min	5.5	$Ce(PO_3)_4$	95.21
24	MW	480 W 10 min	5.5	$Ce(PO_3)_4$	95.96

Table 1 continued

Entries	MW/Calcination condition		*R* value	Products	U(VI) removal rate (%)
25	MW	800 W 5 min	6	$Ce(PO_3)_4$ containing a small amount of impurities	–
26	MW	560 W 10 min	6	$Ce(PO_3)_4$	95.01
27	MW	480 W 10 min	6	$Ce(PO_3)_4$	95.36
28	MW	800 W 5 min	7	$Ce(PO_3)_4$ containing a small amount of impurities	–
29	MW	560 W 10 min	7	$Ce(PO_3)_4$ containing a trace amount of impurities	–
30	MW	480 W 10 min	7	$Ce(PO_3)_4$ containing a trace amount of impurities	–

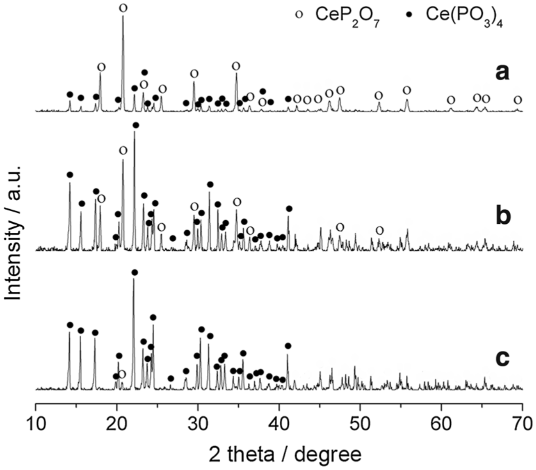

Fig. 2 XRD patterns of samples synthesized at 800 W for 5 min with different *R* values. *a* $R = 2.5$ (entry 5), *b* $R = 3$ (entry 6), *c* $R = 4$ (entry 8)

Results and discussion

Phase analysis

Numerous experiments were performed by changing the parameters molar ratio, reaction time, and MW power. As seen in Fig. 1, the diffraction peaks of $CeH_2P_2O_8$ were observed in the XRD pattern of the sample which was prepared using H_3PO_4 and $Ce(OH)_4$ with $R = 2$ at 800 W for 3 min. H_3PO_4 and $Ce(OH)_4$ thoroughly reacted, and $CeH_2P_2O_8$ transformed into CeP_2O_7 when the reaction time was prolonged to 5 min. All the peaks in Fig. 1a can be indexed to a pure phase, cubic structured CeP_2O_7 [Joint Committee on Powder Diffraction Standards (JCPDS) no.

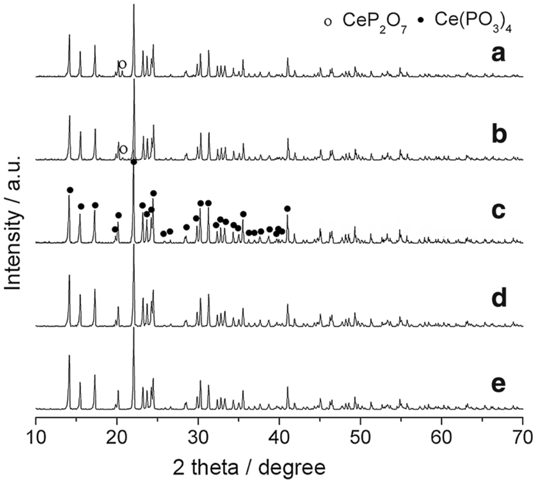

Fig. 3 XRD patterns of samples synthesized at different powers and times when $R = 5$. *a* 800 W 10 min (entry 16), *b* 800 W 5 min (entry 15), *c* 640 W 10 min (entry 17), *d* 560 W 10 min (entry 18), *e* 480 W 10 min (entry 19)

30-0164] [34]. Therefore, synthesizing single-phase CeP_2O_7 at 800 W for 5 min with $R = 2$ is highly suitable (entries 1 and 2 in Table 1) among other many trials.

To investigate the morphology, grain size, and dispersion status of CeP_2O_7 under different conditions [35], an excess amount of H_3PO_4 ($R = 2.5$) was used at 800 W for 5 min. It was found from Fig. 2a, however, the diffraction peaks of $Ce(PO_3)_4$ significantly appeared in the CeP_2O_7 pattern. The diffraction peaks of $Ce(PO_3)_4$ in the XRD pattern of the products (Fig. 2b) became strong when excess H_3PO_4 ($R = 3$) was used at 800 W for 5 min. It is expected that $Ce(PO_3)_4$ was obtained directly by MW irradiation using H_3PO_4 and $Ce(OH)_4$ as raw materials at 800 W for 5 min. Therefore, a stoichiometric reaction between H_3PO_4 and $Ce(OH)_4$ was investigated to obtain a pure $Ce(PO_3)_4$ compound. In this case, when $R = 4$, $Ce(PO_3)_4$ was obtained and small amount of CeP_2O_7 was observed as a side product at a diffraction peak at 20.66°. Moreover, in the same manner, also by keeping $R = 4$ constant and changing the other MW parameters such as 800 W for 3 or 10 min, and 640 W for 5 or 10 min (entries 7–11), the diffraction peak at 20.66° never disappeared. Therefore, pure $Ce(PO_3)_4$ cannot be obtained in the stoichiometric reaction where $R = 4$ regardless of the changes in the reaction conditions.

To synthesize single-phase $Ce(PO_3)_4$ under MW irradiation, experiments in which $R = 5$ under different powers and times were carried out. The CeP_2O_7 phase still existed in the products irradiated at 800 W for 5 or 10 min. However, the CeP_2O_7 diffraction peak at 20.66° disappeared when the reactants were irradiated at

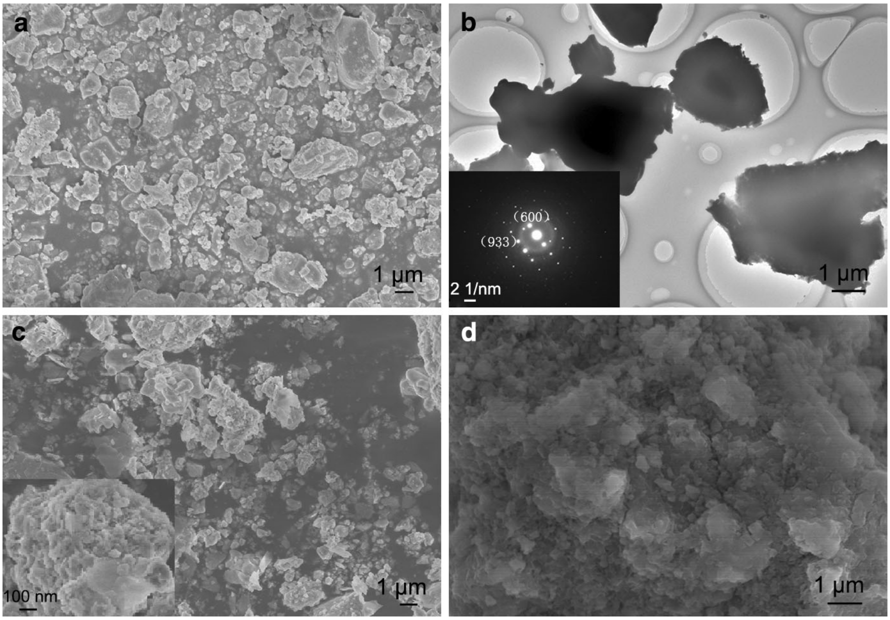

Fig. 4 SEM (**a**) and TEM (**b**) images of CeP_2O_7 synthesized at 800 W for 5 min (entry 2) before U(VI) adsorption, SEM (**c**) image of CeP_2O_7 (entry 2) after U(VI) adsorption, and SEM (**d**) image of CeP_2O_7 synthesized at 300 °C for 60 min (entry 12) before U(VI) adsorption. The *inset* in the TEM image is the SAED patterns of CeP_2O_7 (entry 2)

640, 560, and 480 W for 10 min (Fig. 3). By comparing the obtained data (Fig. 3c, d and e) with the JCPDS no. 25-0188 [36], pure-phase orthorhombic structured $Ce(PO_3)_4$ with a PbCn space group was successfully synthesized by MW irradiation at a low power (640, 560, and 480 W) for 10 min, in which $R = 5$. Additionally, single-phase $Ce(PO_3)_4$ powders were also obtained when $R = 5.5$ and 6. Contrarily, when $R = 7$, single-phase $Ce(PO_3)_4$ powder cannot be synthesized under MW irradiation. As can be seen in Table 1 (entries 15, 16, and 25), a high power is unsuitable for the synthesis of pure $Ce(PO_3)_4$ powders.

For comparison, the reactions were also performed by a conventional heating method. The CeP_2O_7 powder was obtained by calcinating H_3PO_4 and $Ce(OH)_4$ at 300 °C for 60 min when $R = 2$ and 4 (entries 4 and 12 in Table 1). When $R = 5$, a higher temperature (500 °C) and longer time (180 min) were used to obtain $Ce(PO_3)_4$ powders (entry 21).

Both CeP_2O_7 and $Ce(PO_3)_4$ were synthesized using H_3PO_4 as a MW susceptor agent. The possible reaction path of H_3PO_4 under MW irradiation was investigated. Free water was firstly removed from phosphoric acid 85 % under MW irradiation. Subsequently, anhydrous H_3PO_4 was dehydrated to form $H_4P_2O_7$, and then further dehydrated to form HPO_3. The chemical change evidently resulted from the MW effects. H_3PO_4 reacted with $Ce(OH)_4$ to produce the intermediate $CeH_2P_2O_8$ in an active state, and then H_2O was eliminated to form CeP_2O_7. With an increased amount of H_3PO_4, fresh CeP_2O_7 further reacted with H_3PO_4 to form $Ce(PO_3)_4$. This

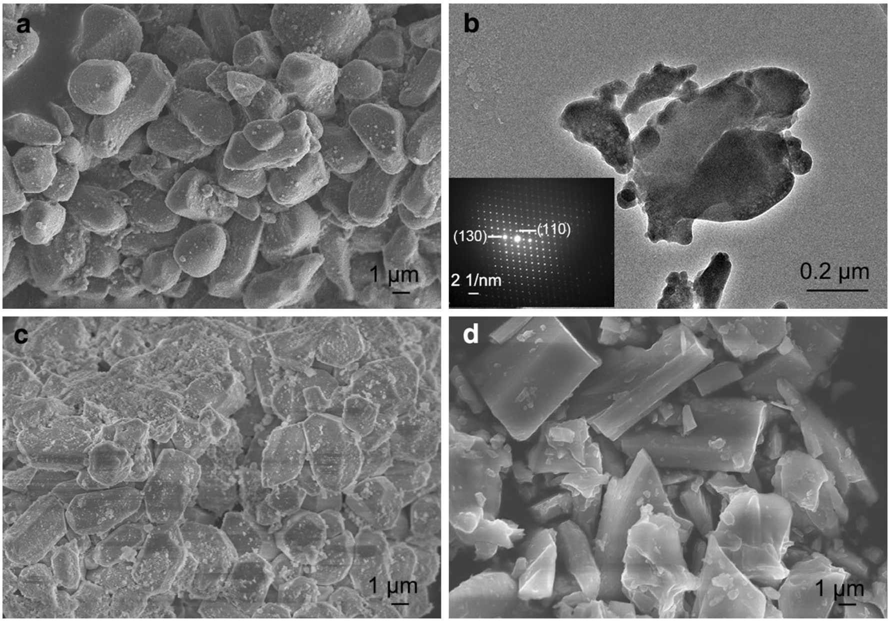

Fig. 5 SEM (**a**) and TEM (**b**) images of $Ce(PO_3)_4$ synthesized at 560 W for 10 min (entry 18) before U(VI) adsorption, SEM (**c**) image of $Ce(PO_3)_4$ (entry 18) after U(VI) adsorption, and SEM (**d**) image of $Ce(PO_3)_4$ synthesized at 500 °C for 180 min (entry 21) before U(VI) adsorption. The *inset* in the TEM image is the SAED patterns of $Ce(PO_3)_4$ (entry 18)

process agreed with the action of H_3PO_4 under MW irradiation. This reaction process can be explained by the following Eq. (1), and the hypothesis is demonstrated in Figs. 1 and 2.

$$2H_3PO_4 + Ce(OH)_4 \xrightarrow{MW} CeH_2P_2O_8 \xrightarrow{-H_2O} CeP_2O_7 \xrightarrow{+H_3PO_4} Ce(PO_3)_4 \quad (1)$$

SEM, TEM and SAED patterns

The SEM, TEM and SAED images of CeP_2O_7 (entry 2) and $Ce(PO_3)_4$ (entry 18) are shown in Figs. 4 and 5. It is suggested that the particles of CeP_2O_7 and $Ce(PO_3)_4$ are irregular in shape and 0.1–3 and 1–5 μm in size, respectively. The insets in Figs. 4b and 5b represent the SAED patterns of as-synthesized CeP_2O_7 and $Ce(PO_3)_4$, indicating that both samples had a monocrystalline structure.

Figures 4c and 5c shows SEM images of CeP_2O_7 (entry 2) and $Ce(PO_3)_4$ (entry 18) after U(VI) adsorption. By contrast with Figs. 4a and 5a, there are comparatively obvious differences between the SEM images before and after U(VI) adsorption. The aggregation of CeP_2O_7 particles (Fig. 4c), the decreasing space between $Ce(PO_3)_4$ particles (Fig. 5c) and rougher surface for both samples are observed. The possible reason is that U(VI) was adsorbed on the surface of both samples. The compact surface of CeP_2O_7 particles prepared at 300 °C for 60 min (entry 12) and angular particles of $Ce(PO_3)_4$ prepared at 500 °C for 180 min (entry 21), which are completely different from CeP_2O_7 and $Ce(PO_3)_4$ gained by MW irradiation (Figs. 4a, 5a), can be observed in Figs. 4d and 5d, respectively.

Adsorption properties of U(VI)

Figure 6 shows the relationship curves of the U(VI) removal rate by CeP_2O_7 (entry 2) and by $Ce(PO_3)_4$ (entry 18) and pH value, contact time, initial concentrations of uranyl ions. It can be seen from Fig. 6a that U(VI) adsorption by both CeP_2O_7 and $Ce(PO_3)_4$ is very sensitive to the pH value and the optimum pH range is 5–7. The removal rate of U(VI) increased sharply within the early 30 min, and then gradually approached equilibrium (Fig. 6b). Figure 6c suggests that the initial concentration had a slight effect on the removal rate of U(VI). To enhance the adsorption capacity of CeP_2O_7 and $Ce(PO_3)_4$ on U(VI), the large initial concentration (1.0 mmol L^{-1})

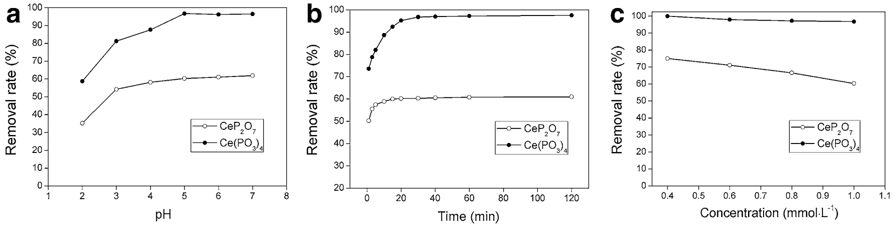

Fig. 6 Effect of pH value (**a**), contact time (**b**), initial concentrations of uranyl ions (**c**) on adsorption of U(VI) on CeP_2O_7 (entry 2) and $Ce(PO_3)_4$ (entry 18)

Table 2 Kinetic parameters for U(VI) adsorption onto CeP_2O_7 and $Ce(PO_3)_4$

Adsorbents	$q_{e,\mathrm{exp}}$ (mg g^{-1})	Pseudo-first-order equation			Pseudo-second-order equation			Intraparticle diffusion	
		$k_1 \times 10^{-2}$ (min^{-1})	$q_{e,\mathrm{cal}}$ (mg g^{-1})	R^2	$k_2 \times 10^{-3}$ (g mg^{-1} min^{-1})	$q_{e,\mathrm{cal}}$ (mg g^{-1})	R^2	k_{dif} (mg g^{-1} min$^{-1/2}$)	R^2
CeP_2O_7	164.5	6.19	13.44	0.951	18.83	165.0	0.999	2.16	0.47
$Ce(PO_3)_4$	263.4	7.39	45.27	0.969	5.26	265.3	0.999	6.44	0.636

was used in the current experiment. Therefore, the following discussed adsorption of U(VI) on a series of cerium phosphates listed in Table 1 was achieved at a pH of 5, within 30 min and at an initial concentration of 1.0 mmol L^{-1}.

Compared to entries 5, 6, 8 and 15 in Table 1, it can be discerned that the removal rate of U(VI) increases with the increasing of $Ce(PO_3)_4$ content in the obtained mixtures of CeP_2O_7 and $Ce(PO_3)_4$. This can be proved from Fig. 6 and by comparing entries 2–18 in Table 1. It is implied that U(VI) is adsorbed on $Ce(PO_3)_4$ more effectively than CeP_2O_7. It might be mainly attributable to different sorption sites probably formed by the oxygens of the PO_3 and P_2O_7 surface groups, and a difference in the number of $\equiv$ P–O sites resulted from distinct P/Ce molar ratios between $Ce(PO_3)_4$ and CeP_2O_7. By contrast, the removal rate of CeP_2O_7 and $Ce(PO_3)_4$ obtained by calcinations on U(VI) are significantly lower than those synthesized under MW irradiation. The possible reason is that far more time was required to obtained products at high temperatures by the calcination method than MW irradiation, which resulted in the agglomeration and sintering of particles in the calcinated products.

In order to evaluate the controlling mechanism of the adsorption process, three kinetic models, namely the pseudo-first-order model, pseudo-second-order model and the intraparticle diffusion model were tested to interpret the data obtained from the batch experiments. These three models can be expressed by the following Eqs. (2)–(4), respectively [37].

$$\log(q_e - q_t) = \log q_e - \frac{k_1}{2.303} \times t \tag{2}$$

$$\frac{t}{q_t} = \frac{1}{k_2 q_e^2} + \frac{t}{q_e} \tag{3}$$

$$q_t = k_3 t^{0.5} + I \tag{4}$$

where q_e and q_t (mg g^{-1}) are the amount of ${UO_2}^{2+}$ adsorbed at the equilibrium state and time t. k_1 (min^{-1}), k_2 (g mg^{-1} min^{-1}) and k_3 (mg g^{-1} $min^{-1/2}$) are the pseudo-first-order, the pseudo-second-order and the intraparticle diffusion rate constants, respectively. I (mg g^{-1}) is the constant.

k_1, k_2, k_3, q_e, and the correlative coefficient R^2 of three kinetic models were obtained from plots of $\log(q_e - q_t)$ versus t, t/q_t versus t and q_t versus $t^{1/2}$, via linear regression of experimental data. As presented in Table 2, the higher correlative coefficient R^2 and correlation value with the $q_{e,\mathrm{cal}}$ closer to the experimental adsorption capacity $q_{e,\mathrm{exp}}$ suggested that the pseudo-second order kinetic model could be fit to descript the adsorption process. It is implied that this adsorption process might be considered as chemisorption which is the rate-controlling step [37].

Conclusions

Different products can be obtained through a green (i.e., environmentally friendly) route using different mole ratios of H_3PO_4 to $Ce(OH)_4$ as raw materials under MW irradiation. When the mole ratio of H_3PO_4 to $Ce(OH)_4$ is equal to 2 and 2.5–4, monophase CeP_2O_7 and the mixture including CeP_2O_7 and $Ce(PO_3)_4$ could be synthesized at 800 W for 5 min under MW irradiation, respectively. Under MW irradiation condition, monophase $Ce(PO_3)_4$ can be obtained at a low power of 480 W for 10 min in the presence of a chemometric excess of H_3PO_4 ($R = 5$–6). The particle sizes of the as-synthesized CeP_2O_7 ranged from 0.1 to 3 μm, whereas those of $Ce(PO_3)_4$ ranged from 1 to 5 μm, as observed in SEM and TEM images. The kinetics analysis suggested that chemisorption was the rate-controlling step in the adsorption process of CeP_2O_7 and $Ce(PO_3)_4$ for U(VI). Differences of adsorption site and the P/Ce molar ratio between CeP_2O_7 and $Ce(PO_3)_4$ are possible reasons for their different adsorption abilities on U(VI). Both CeP_2O_7 and $Ce(PO_3)_4$ synthesized under MW irradiation are promising adsorbents for the efficient removal of U(VI) from aqueous solutions, and their removal rates are markedly better than those of CeP_2O_7 and $Ce(PO_3)_4$ obtained by calcination of H_3PO_4 (85 %) and $Ce(OH)_4$. Therefore, the proposed technique was effective and environmentally friendly for the synthesis of CeP_2O_7 and $Ce(PO_3)_4$, and has potential future applications.

Acknowledgments This work was supported by the National Natural Science Foundation of China (21276046 and 21406045), the Natural Science Foundation of Liaoning Province (2015020199), the Fundamental Research Funds for the Central Universities of China (DUT14LK32), and the Scientific Research Project of the Education Department of Liaoning Province (L2012134).

References

1. S. Chall, S.S. Mati, S. Rakshit, S.C. Bhattacharya, J. Phys. Chem. C **117**, 25146 (2013)
2. A. Phuruangrat, N. Ekthammathat, S. Thongtem, T. Thongtem, Res. Chem. Intermed. **39**, 1363 (2013)
3. M.V. Le, D.S. Tsai, C.Y. Yang, W.H. Chung, H.Y. Lee, Electrochim. Acta **56**, 6654 (2011)
4. T. Parangi, B. Wani, U. Chudasama, Electrochim. Acta **148**, 79 (2014)
5. B. Singh, J.H. Kim, S.Y. Jeon, J.Y. Park, S.J. Song, J. Electrochem. Soc. **161**, F133 (2014)
6. C. Chatzichristodoulou, J. Hallinder, A. Lapina, P. Holtapples, M. Mogensen, J. Electrochem. Soc. **160**, F798 (2013)
7. H. Onoda, H. Nariai, A. Moriwaki, H. Maki, I. Motooka, J. Mater. Chem. **12**, 1754 (2002)
8. I.C. Marcu, I. Sandulescu, J.M.M. Millet, Appl. Catal. A Gen. **227**, 309 (2002)
9. J. Kang, S. Byun, S. Nam, S. Kang, T. Moon, B. Park, Int. J. Hydrogen Energy **39**, 10921 (2014)
10. T. Parangi, B. Wani, U. Chudasama, Appl. Catal. A Gen. **467**, 430 (2013)
11. S.L. Zhong, L.F. Luo, L. Wang, L.F. Zhang, Powder Technol. **230**, 151 (2012)
12. N. Imanaka, T. Masui, H. Hirai, G. Adachi, Chem. Mater. **15**, 2289 (2003)
13. V.C. Seixas, O.A. Serra, Molecules **19**, 9907 (2014)
14. J.F. de Lima, O.A. Serra, Dyes Pigments **97**, 291 (2013)
15. K.M. White, P.L. Lee, P.J. Chupas, K.W. Chapman, E.A. Payzant, A.C. Jupe, W.A. Bassett, C.S. Zha, A.P. Wilkinson, Chem. Mater. **20**, 3728 (2008)
16. R. Asuvathraman, K.V.G. Kutty, Thermochim. Acta **581**, 54 (2014)
17. E. Ordoñez-Regil, R. Drot, E. Simoni, J. Colloid Interface Sci. **263**, 391 (2003)
18. R. Drot, E. Simoni, M. Alnot, J.J. Ehrhardt, J. Colloid Interface Sci. **205**, 410 (1998)
19. P. Zeng, Y.C. Teng, Y. Huang, L. Wu, X.H. Wang, J. Nucl. Mater. **452**, 407 (2014)
20. L.A. Boatner, B.C. Sales, in *Radioactive Waste Forms for the Future*, ed. by W. Lutze, R.C. Ewing (Elsevier, Amsterdam, 1988), p. 495
21. N. Clavier, E.D.F. de Kerdaniel, N. Dacheux, P.L. Coustumer, R. Drot, J. Ravaux, E. Simoni, J. Nucl. Mater. **349**, 304 (2006)
22. R. Drot, C. Lindecker, B. Fourest, E. Simoni, New J. Chem. **22**, 1105 (1998)
23. V. Brandel, N. Dacheux, E. Pichot, M. Genet, Chem. Mater. **10**, 345 (1998)

24. N. Dacheux, B. Chassigneux, V. Brandel, P.L. Coustumer, M. Genet, G. Cizeron, Chem. Mater. **14**, 2953 (2002)
25. P. Bénard, V. Brandel, N. Dacheux, S. Jaulmes, S. Launay, C. Lindecker, M. Genet, D. Louër, M. Quarton, Chem. Mater. **8**, 181 (1996)
26. P. Bénard, D. Louër, N. Dacheux, V. Brandel, M. Genet, Chem. Mater. **6**, 1049 (1994)
27. H.A. Höppe, M. Daub, Z. Kristallogr. **227**, 535 (2012)
28. Y.H. Lai, Y.C. Chang, T.F. Wong, W.J. Tai, W.J. Chang, K.H. Lii, Inorg. Chem. **52**, 13639 (2013)
29. H. Onoda, Y. Inagaki, A. Kuwabara, N. Kitamura, K. Amezawa, A. Nakahira, I. Tanaka, J. Ceram. Process. Res. **11**, 344 (2010)
30. T. Masui, H. Hirai, N. Imanaka, G. Adachi, Phys. Stat. Sol. A **198**, 364 (2003)
31. M. Tsuhako, S. Ikeuchi, T. Matsuo, I. Motooka, M. Kobayashi, Chem. Lett. **6**, 195 (1977)
32. P. Michard, E. Guibal, T. Vincent, P. Le Cloirec, Microporous Mater. **5**, 309 (1996)
33. E. Guibal, I. Saucedo, J. Roussy, P. Le Cloirec, React. Polym. **23**, 147 (1994)
34. I.L. Von Botto, E.J. Baran, Kristallographische daten Z. Anorg. Allg. Chem. **430**, 283 (1977)
35. R. Wang, J.W. Ye, G.L. Ning, H. Jiang, W.L. Zhou, F.H. Sun, Mater. Lett. **83**, 130 (2012)
36. R. Masse, J.C. Grenier, Bull. Soc. Fr. Minéral. Cristallogr. **95**, 136 (1972)
37. S.A. Sadeek, M.A. El-Sayed, M.M. Amine, M.O. Abd. El-Magied, J. Radioanal. Nucl. Chem. **299**, 1299 (2014)